International Journal of Engineering Research & Technology (IJERT)
ISSN: 2278-0181
Vol. 4 Issue 04, April-2015

De-noising with Different Bi-orthogonal Spline Wavelets using DWT

T. N. Tilak & S Krishnakumar
School of Technology & Applied Sciences
Mahatma Gandhi University
Kochi-24, India

***Abstract*—This paper examines the de-noising performance of the different bi-orthogonal spline wavelets, making use of Discrete Wavelet Transform. We investigate the dependence of the peak signal to noise ratio of the de-noised images on the filter properties of the bi-orthogonal wavelets used in the DWT. The bi-orthogonal spline wavelet most suited for de-noising application has been sorted out.**

Key words - Bi-orthogonal spline wavelet, discrete wavelet transform, AWGN, thresholding.

I. INTRODUCTION

The classical frequency domain image de-noising processes make use of the Fourier Transform for the decomposition and reconstruction processes. The basis function of the Fourier transform is $e^{-j\omega t}$ which results in a sinusoidal decomposition of the image. But Fourier analysis provides only a single resolution always. If we choose a coarse resolution we lose the small details in the image; if a small resolution is chosen we lose the large structures in the image. This problem can be circumvented by making use of Wavelet Transform for the analysis, instead of Fourier Transform. Wavelet transform can break up any data in to different frequency components and then study each component with a resolution that matches its scale[1]. Thus "multi-resolution analysis"(MRA),i.e., analyzing different frequency components at different resolutions becomes possible. Thus one can see the finer and coarse details in an image [2]. A selected "wavelet" forms the basis function in a Wavelet Transform. The families of the function

$$h_{a,b}(x) = |a|^{-\frac{1}{2}} h\left(\frac{x-b}{a}\right), \quad (1)$$

$a, b \varepsilon R, a \neq 0$, generated from one single function 'h' by dilations and translations of the function are called wavelets [3]. The function which is subjected to dilations and translations is called the "Mother wavelet". The basis function which has zero value outside a finite interval is said to have a "compact support". This characteristic which stands for a fast decay as the time tends to infinity is useful in providing the wavelet analysis time and frequency localization. Such compactly supported wavelet bases have FIR filters with perfect reconstruction [4].

The performance of the different members of a family of wavelets called "bi-orthogonal spline wavelets", in de-noising using Discrete Wavelet Transform (DWT) is discussed in this paper.

II. MATERIALS AND METHODS

A. Bi-orthogonal wavelets

A bi-orthogonal wavelet is a combination of two wavelets. Out of these two wavelets, one wavelet is used for decomposition and the other is used for reconstruction. Symmetry and exact reconstruction cannot be achieved simultaneously if we use one and the same wavelet for decomposition and reconstruction. Bi-orthogonal wavelets help to overcome this problem. The term "bi-orthogonal" indicates that the individual wavelets in the bi-orthogonal wavelet need not be orthogonal but that they are pair-wise orthogonal.

Two functions f(x) and g(x) are said to be orthogonal if :

$$\int f(x) g^*(x) = 0, \quad (2)$$

where $g^*(x)$ is the conjugate of g(x). Bi-orthogonality (and orthogonality) makes the computations speedy and easy. In addition, bi-orthogonal wavelets exhibit linear phase property which is highly desirable for image reconstruction [5]. The bi-orthogonal spline wavelets are symbolically represented as 'bior Nr.Nd' where Nr and Nd stand for the number of vanishing moments in the reconstruction wavelet and the decomposition wavelet respectively. A wavelet Ψ is said to have p vanishing moments if:

$$\int x^k \Psi dx = 0, \quad (3)$$

where p = 0,1,..k-1[6]. If the number of vanishing moments is large, it implies that its "support" or equivalently the "filter length" is large. The bi-orthogonal spline wavelets which satisfy compact support and perfect reconstruction with FIR filters are: 'bior 1.1', 'bior 1.3', 'bior 1.5', 'bior 2.2', 'bior 2.4', 'bior 2.6', 'bior 2.8','bior 3.1', 'bior 3.3', 'bior 3.5', 'bior 3.7', 'bior 3.9', 'bior 4.4', 'bior 5.5' and 'bior 6.8'. DWT using each of these bi-orthogonal wavelets are successively employed in our study.

B. Addition of noise

The most common noise encountered in digital images is the Additive White Gaussian Noise (AWGN) [7]. Hence we employ AWGN as the noise in the image used for the study. The model used to describe AWGN is:

$$w(u,v) = s(u,v) + n(u,v), \quad (4)$$

where $w(u,v)$ represents any picture element (pixel) in the noisy image, $s(u,v)$ is the true value of the element and $n(u,v)$ is the random Gaussian noise value [8]. First we add an AWGN with variance σ^2 = 0.07 in a 0-1 scale, to the original image, to produce a corrupted image. Here we have

employed a comparatively high noise value to ensure good visual comparison of the resultant images with the noisy image.

C. Levels of Decomposition.

The decomposition using DWT can be performed repeatedly until the last detail components have only a single pixel. But we may limit the levels of decomposition to such a value determined by criteria such as noise level of the image and the acceptability of the reconstructed image. The results of a pilot study conducted by the authors indicated that only a low amount of noise gets removed with one or two levels of decomposition and that four or more levels of decomposition result in blurring due to removal of more information. Hence in this study we adopt an optimum of three levels of decomposition.

D. Thresholding.

The de-noising process basically comprises the following strategy:

1. Decompose the noisy image. This results in generation of a number of coefficients.
2. Adopt an appropriate threshold strategy and apply the threshold function to the coefficients.
3. Reconstruct the image from the coefficients that remain after application of the threshold.

Hence any wavelet based de-noising operation requires selection of a proper threshold criterion. Careful selection of threshold is important because, a large threshold value may result in blurring, and a small threshold removes little noise [9]. 'Hard thresholding' and 'soft thresholding' are the two major thresholding techniques usually adopted. Hard thresholding involves complete elimination of coefficients whose values are below the threshold value. But in soft thresholding, in addition to elimination of those coefficients whose values fall below the threshold, we shrink the remaining coefficients towards zero. This strategy precludes occurrence of sharp discontinuities in the reconstructed image. Soft thresholding has been observed to give better results than hard thresholding and is hence preferred to the other [10]. This fact has made us choose soft thresholding for our work.

The value of the threshold as determined by "Fixed form threshold" given in Matlab and originally proposed by Donoho and Johnstone [11], defined as:

$$d = \sigma \sqrt{2 \log M}, \qquad (5)$$

where d is the threshold value, σ is standard deviation of noise and M is the size of the image, is used for our study.

E. Performance measures

The factors used to assess the effectiveness of de-noising performance are the Mean Squared Error (MSE) and Peak Signal to Noise Ratio (PSNR). These two parameters are calculated using the following formulae :

$$MSE = \frac{1}{m\,n} \sum_{i=1}^{m} \sum_{j=1}^{n} (X(i,j) - X'(i,j))^2 \qquad (6)$$

$$PSNR = 10 \log \left(\frac{255^2}{MSE} \right) \text{ dB}, \qquad (7)$$

where X is the original image and X′ is the denoised image [12]. Also. the quality of the de-noised images are compared by means of physical observation since there exists no other consensual method for comparison of visual quality of de-noised images [13].The whole study described in this paper has been carried out using Matlab.

F. Procedure:

An image of such size permitting at least three levels of decomposition is selected. The image 'lena' of size [512, 512] is one such image. AWGN of variance 0.07 (in 0 – 1 scale) is added to this image to produce a noisy image. De-noising of this noisy image is carried out with DWT using 'bior1.1" wavelet. The performance factors mentioned in section II E are estimated and tabulated. The effective lengths, filter values and the minimum and maximum filter values of the high pass and low pass decomposition and reconstruction filters are estimated and recorded. All the above operations are repeated with the same noisy image for the other bi-orthogonal wavelets listed in section II A also, successively. Since quadrature mirror filter relationship exists between the high pass reconstruction filters and the low pass decomposition filters and also between the high pass decomposition filters and the low pass reconstruction filters of the individual bi-orthogonal wavelets, the maximal and minimal values of only the high pass reconstruction filter and high pass decomposition filter have been shown in this paper. The results are analyzed to explore how the de-noising performance of the different bi-orthogonal spline wavelets are related to the respective values of the decomposition and reconstruction filters.

III. Results and Discussion

Fig.1 shows the original noise-less image. Fig.2 is the noisy image. Fig.3 shows the de-noised image having the highest PSNR and Fig.4 shows the de-noised image having the lowest PSNR. Table1 shows the estimated values of PSNR and MSE corresponding to the different de-noising processes i.e., using the different bi-orthogonal wavelets. The last four columns of this table show the effective lengths of the low pass decomposition filter (Lo_D), high pass decomposition filter (Hi_D), low pass reconstruction filter (Lo_R) and the high pass reconstruction filter (Hi_R) in the order said, from left to right. Table 2 shows the maximum and minimum values of the high pass decomposition filters and the high pass reconstruction filters. The low pass filter outputs give an approximation of the image. The high pass decomposition filter Hi_D and the high pass reconstruction filter Hi_R take care of the high frequency parts of the image; as such they operate on the noise part of the image.

The values of PSNR (and also the MSE) of the de-noised images vary for de-noising carried out using the different bi-orthogonal wavelets.

From table 1, we can see that the maximum value of PSNR is obtained by de-noising using the bi-orthogonal wavelet 1.1 ('bior'1.1). In this case the wavelets used for both decomposition and reconstruction are one and the same. The corresponding filters are also identical. Figs. 5(i) and 5(ii) show these wavelets and the corresponding filters respectively. Here we see that Hi_R (and also Hi_D in this particular case) has the minimum length,'2'. The next de-noising process makes use of 'bior1.3' wavelet; it gives a lower PSNR and has a longer Hi_R. Similarly, a comparison of the other values of PSNR and the lengths of the filters given in table1 shows that changes in the PSNR values with de-noising using the different bi-orthogonal


Fig.1. Original image


Fig.2. Noisy image

wavelets can be related to the changes in the effective lengths of the filters Hi_R and Hi_D of the bi-orthogonal wavelets. It can be seen that the PSNR has an inverse relation to the effective length of Hi_R. When the effective lengths of Hi_R are equal, a similar inverse relation is found to exist between the PSNR and the effective lengths of Hi_D. A few exceptions are noted in relation to the former of these observations:

1. The first exception is found when we move from 'bior 2.2' to 'bior 2.4'. Here effective length of Hi_R changes from 5 to 9 but there is a very slight increase in the PSNR. This contradiction is explained as follows: The values of Hi_R for 'bior2.2' are:

Hi_R ('bior2.2') = [0 0.1768 0.3536 -1.0607 0.3536 0.1768] and the values of Hi_R for 'bior2.4' are:

Hi_R ('bior2.4') = [0 -0.0331 -0.0663 0.1768 0.4198 -0.9944 0.4198 0.1768 -0.0663 -0.0331]. It can be seen that even though the length of Hi_R for 'bior2.2' is less than that of 'bior 2,4', the filter values of 'bior 2.4' are mostly very small compared to the values of 'bior 2.2'. Relating the effect of Hi_R on the noise in the reconstructed image we can say that due to the filter values of 'bior 2.4' being very small the noise components accumulated by the filter Hi_R is very small, the decreasing effect on PSNR due to the increase in length of filter Hi_R is countered and to some extent reversed, thus resulting in an actual slight increase in the PSNR.

2. Another exception is encountered when we pass from 'bior2.8' to 'bior3.1'. The reason for this is:

Examining table 2 we can see that the maximum value of Hi_R has increased from 0.4626 to 1.0607. This is an increase of 129.29%. Simultaneously Hi_R minimum has decreased from -0.9516 to -1.0607. This is a decrease of 11.46%. Both of these together have the effect of carrying a good amount of noise in to the reconstructed image. Hence even though the effective length of Hi_R has faced a reduction, the PSNR has undergone a drastic reduction, instead of augmentation. The increase in the effective length of Hi_D has augmented this reduction in PSNR. In effect, with 'bior3.1', we get the minimum PSNR.

Since 'bior 3.1' gives odd values it is better to treat de-noising with 'bior 3.1' as of little use compared to the other bi-orthogonal wavelets. Hence the de-noising performance of


Fig.3.Image with highest PSNR


Fig.4. Image with lowest PSNR

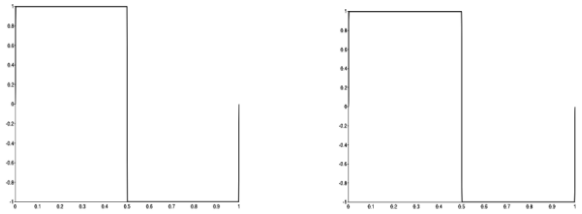

Fig.(5i).(a) Decomposition wavelet and (b) reconstruction wavelet of 'bior 1.1'

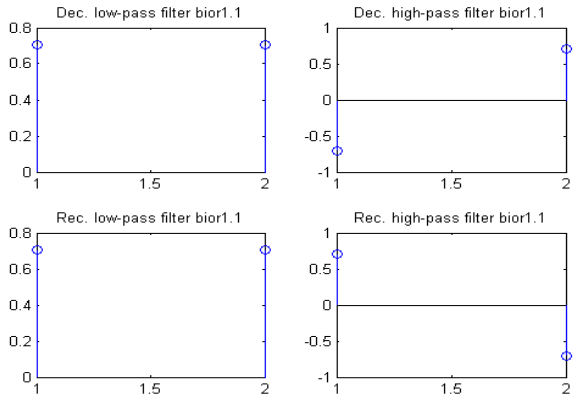

Fig. 5(ii) Filters of 'bior 1.1 '

'bior 3.3' is examined in comparison with that of 'bior 2.8' instead of comparing with the performance of 'bior 3.1'.

3. It can be seen that the effective length of Hi_R of 'bior 3.3' is lower than that of 'bior 2.8'; the PSNR is also lower for 'bior3.3'. This is due to the following facts: even though the effective length of Hi_R is lesser in the case of 'bior 3.3', the maximum value of Hi_R has increased and the minimum value of Hi_R has decreased, resulting in a combined effect of retaining a high amount of noise in the reconstructed image and consequently giving a lower PSNR.

4. The effective length of Hi_R is longer for 'bior3.5' but the PSNR is higher, compared to that of 'bior 3.3'. This is explained in the discussion below.

The values of Hi_R for 'bior 3.3' are:

Hi_R ('bior3.3') = [0.0663 0.1989 -0.1547 -0.9944 0.9944 0.1547 -0.1989 -0.0663] and the values of Hi_R for 'bior 3.5' are:

Hi_R ('bior3.5') = [-0.0138 -0.0414 0.0525 0.2679 -0.0718 -0.9667 0.9667 0.0718 -0.2679 -0.0525 0.0414 0.0138]. It can be seen that the values of Hi_R of 'bior 3.5' are very meagre compared to those of 'bior 3.3'.This results in lesser noise being carried on to the reconstructed image and hence in a higher PSNR.

5. When we consider de-noising using 'bior 3.7', it is seen that the effective length is higher than that of 'bior 3.5' but that the corresponding PSNR is also higher. But this is due to the fact that, as seen from table 2, the maximum value of Hi_R has decreased and minimum value of Hi_R has increased.

In de-noising with all other bi-orthogonal wavelets it can be seen that the PSNR has an inverse relation to the effective length of Hi_R. The maximum PSNR is obtained by de-noising using the bi-orthogonal wavelet having minimum length for Hi_R. But the inverse of this statement is not true because, like what has been found in several instances pointed out above, the PSNR is also affected by the actual values of the filter, rather than its length only. Further to the above, it is also found that in instances in which the effective lengths of Hi_R are equal, the

TABLE 1.

Wavelets, MSE, PSNR and Effective lengths of filters						
Ψ	***MSE***	***PSNR***	***Effective Lengths of Filters***			
			Lo_D	***Hi_D***	***Lo_R***	***Hi_R***
bior1.1	29.0779	33.4952	2	2	2	2
bior1.3	30.1858	33.3328	6	2	2	6
bior1.5	30.4096	33.3007	10	2	2	10
bior2.2	29.1871	33.4789	5	3	3	5
bior2.4	29.1807	33.4798	9	3	3	9
bior2.6	29.2937	33.4631	13	3	3	13
bior2.8	29.3623	33.4529	17	3	3	17
bior3.1	33.9804	32.8185	4	4	4	4
bior3.3	29.8271	33.3847	8	4	4	8
bior3.5	29.4298	33.4429	12	4	4	12
bior3.7	29.2377	33.4714	16	4	4	16
bior3.9	29.4003	33.4473	20	4	4	20
bior4.4	29.1761	33.4805	9	7	7	9
bior5.5	29.3074	33.4610	9	11	11	9
bior6.8	29.4075	33.4462	17	11	11	17

TABLE 2

Wavelets and Extremities of Filter values				
Ψ	***Hi_D min***	***Hi_D max***	***Hi_R min***	***Hi_R max***
bior1.1	-0.7071	0.7071	-0.7071	0.7071
bior1.3	-0.7071	0.7071	-0.7071	0.7071
bior1.5	-0.7071	0.7071	-0.7071	0.7071
bior2.2	-0.7071	0.3536	-1.0607	0.3536
bior2.4	-0.7071	0.3536	-0.9944	0.4198
bior2.6	-0.7071	0.3536	-0.9667	0.4475
bior2.8	-0.7071	0.3536	-0.9516	0.4626
bior3.1	-0.5303	0.5303	-1.0607	1.0607
bior3.3	-0.5303	0.5303	-0.9944	0.9944
bior3.5	-0.5303	0.5303	-0.9667	0.9667
bior3.7	-0.5303	0.5303	-0.9516	0.9516
bior3.9	-0.5303	0.5303	-0.9421	0.9421
bior4.4	-0.7885	0.4181	-0.8527	0.3774
bior5.5	-0.4768	0.8995	-0.3456	0.7367
bior6.8	-0.7589	0.4178	-0.8259	0.4208

PSNR has an inverse relation to the effective lengths of Hi_D.

What has been said above looks in to the relationship of PSNR got by de-noising making use of the different bi-orthogonal wavelets, to the difference in the high pass filters' values and lengths.

Apart from the PSNR values, visual inspection of the de-noised images reveals that all of them have artifacts. This is due to the inherent feature of DWT that it is not shift-invariant. This means that the DWT of a time-shifted signal or image is not the same as the DWT of the original signal This problem can be resolved by employing Shift-invariant Wavelet Transform (SWT) for de-noising. However, our emphasis is on studying the relative performance of the different bi-orthogonal spline wavelets in de-noising.

IV. CONCLUSION

This paper presents an investigation of the denoising performance of the different bi-orthogonal spline wavelets, using DWT. The results show that the denoising performance improves as the effective length of the highpass reconstruction filter or the effective length of the high pass decomposition filter decreases. The maximum value of PSNR and correspondingly the best de-noising performance is obtained with the bi-orthogonal wavelet 'bior 1.1'. Hence 'bior 1.1' is most suitable for de-noising. The bi-orthogonal wavelet 'bior 3.1' gives the worst de-noising performance and is not at all suitable for de-noising purpose. The de-noising performance of the other bi-orthogonal spline wavelets lie in between these two extremes.

REFERENCES

[1] Ingrid Daubechies, Ten Lectures On Wavelets. SIAM, 1992.

[2] M. Gonzalez, X. Otasu , O. Fors and A. Seco, "Comparison betweenMallat's and the 'a` trous' discrete wavelet transform based algorithms for the fusion of multispectral and panchromatic images", International Journal of Remote Sensing Vol. 000, No. 000, Month 2005, 1–19

[3] Ingrid Daubechies, Orthonormal Bases of Compactly Supported Wavelets, Communications on Pure and Applied Mathematics, Vol. XLI 909-996 (1988) John Wiley & Sons, Inc. 1988, CCC 0010-3640/88/070909-88.

[4] Martin Vetterli and Connac Herley, Wavelets and Filter Banks: Theory and Design, IEEE Transactions on Signal Processing, Vol.40, No. 9, September 1992.

[5] Krishna Kumar, Basant Kumar & Rachna Shah, Analysis of Efficient Wavelet Based Volumetric Image Compression, International Journal of Image Processing *(*IJIP*)*, Volume (6) : Issue (2) : 2012, 113 – 122

[6] Myung-Sin Song, Wavelet Image Compression, Contemporary Mathematics1991 Mathematics Subject Classification. Primary 42C40.

[7] Lovely Passrija Amardeep Singh Virk Mandeep Kaur, Performance Evaluation of Image Enhancement Techniques in Spatial and Wavelet Domains, International Journal of Computers & TechnologyVolume 3, No. 1, AUG, 2012.

[8] Jyotsna Patil1, Sunita Jadhav, A Comparative Study of Image Denoising Techniques, International Journal of Innovative Research in Science, Engineering and Technology Vol. 2, Issue 3, March 2013

[9] Priyadharshini, Gayathri, Priyanka and Eswari "Image Denoising Based On Adaptive Wavelet Multiscale Thresholding Method', International Journal of Science and Modern Engineering, Issue5, April 2013.

[10] Grace Chang, Bin Yu, and Martin Vetterli, Adaptive Wavelet Thresholding for Image Denoising and Compression, IEEE Transactions on Image processing, Vol.9,No.9, September 2000.

[11] Mantosh Biswas and Hari Om, An Image Denoising Threshold Estimation Method, Advances in Computer Science and its Applications (ACSA),Vol. 2, No. 3, 2013.

[12] Hari Om, Mantosh Biswas, An Improved Image Denoising Method Based on Wavelet Thresholdin, Journal of Signal and Information Processing, 2012, 3, 109-116 B65.

[13] Florian Luisier, Thierry Blu, and Michael Unser, A New SURE Approach to Image Denoising: Interscale Orthonormal Wavelet Thresholding, IEEE Transactions on Image Processing, Vol.16, No.3, March 2007.